A Review of Wave Energy Converters for Stabilisation and Power Output Optimisation of Floating Offshore Wind Platforms

Josefredo Gadelha da Silva, Marcio J. Lacerda, and Erivelton Nepomuceno

***Abstract*—Hybrid wind-wave systems, which integrate floating offshore wind turbines with wave energy converters, have emerged as a promising solution for enhancing the stability and energy efficiency of offshore renewable platforms. This review explores recent advances in the use of wave energy converters and control strategies aimed at improving platform motion suppression, structural load mitigation, and power production within hybrid wind-wave systems. Particular emphasis is placed on the dynamic coupling between wind and wave subsystems, with a focus on co-optimised control approaches that leverage the power take-off of wave energy converters to support traditional wind turbine control mechanisms. The review includes an overview of classical wind turbine control, passive damping techniques such as tuned mass dampers, and recent methodologies that combine conventional wind turbine controllers with power take-off control systems. Additionally, a comparative summary of typical hybrid wind-wave systems topologies and control architectures is presented.**

***Index Terms*—Floating offshore wind platforms, Wave Energy Converters, Renewable Energy, Control.**

I. Introduction

THE traditional control problem of Wind Turbines (WTs) relies on two main control mechanisms: generator torque control and blade pitch control. Below the rated wind speed, the controller adjusts the generator torque based on a cubic law to maximize power extraction by maintaining the optimal tip-speed ratio. Once the turbine reaches its rated speed, a Proportional-Integral (PI) controller is activated to regulate the blade pitch angle, limiting aerodynamic power and ensuring that the turbine does not exceed its rated power output [1]. This approach, while effective for standard WT operations, relies on predefined control laws and lacks adaptability to external disturbances, making it less efficient in complex environments such as Floating Offshore Wind Turbines (FOWTs), where additional stabilization mechanisms may be required.

This publication has emanated from research conducted with the financial support of Taighde Éireann – Research Ireland under Grant number 21/FFP-P/10065. For the purpose of Open Access, the author has applied a CC BY public copyright licence to any Author Accepted Manuscript version arising from this submission. Erivelton Nepomuceno was supported by Brazilian Research Agency CNPq (Grant No. 444154/2024-8).

Silva, J. G. D. is with the Centre for Ocean Energy Research, Department of Electronic Engineering, Maynooth University, Maynooth, Ireland (e-mail: josefredo.silva.2024@mumail.ie).

Lacerda, M. J. is with the School of Computing and Digital Media, London Metropolitan University, London, UK (e-mail: m.lacerda@londonmet.ac.uk).

Nepomuceno, E. is with the Hamilton Institute and the Centre for Ocean Energy Research, Department of Electronic Engineering, Maynooth University, Maynooth, Ireland. (e-mail: erivelton.nepomuceno@mu.ie).

Floating offshore wind turbines have recently been adopted as a more economical solution for deep waters compared to fixed-bottom wind turbines [2]. Additionally, recent advancements in the control of FOWTs, considering stability challenges, include the development of the commonly used Reference Open-Source Controller (ROSCO) [3]. This controller integrates a floating feedback mechanism that enhances pitch control by adjusting it based on tower-top acceleration signals, thereby improving FOWT stability. Additionally, ROSCO employs more advanced control strategies, such as optimal gain scheduling and state-based adaptations, offering significant improvements over the traditional Baseline WT Controller [4].

On the other hand, hybridization and co-location have been widely explored with the dual objective of mitigating the effects of wave excitation frequencies on floating platform motion and maximizing the potential of integrating different energy sources [5], [6]. This approach is particularly compelling, as wind and wave energy are among the most promising renewable technologies in the energy sector [7], [8].

Firstly, as wave energy remains in the early stages of development compared to offshore wind energy, there is an opportunity to lower its Levelized Cost of Energy (LCOE) by integrating infrastructure with the more established offshore wind technology. Integrating multiple Wave Energy Converters (WECs) with FOWTs substantially reduces costs associated with the WEC's steel frame, mooring system, electrical transmission lines, and siting/permitting, which can comprise up to 56% of the total cost of a standalone WEC [9].

Additionally, this synergy helps mitigate structural loads in FOWTs. Common challenges arise from wave- and wind-induced oscillations, which generate undesirable loads on the blades, rotor shaft, yaw bearing, and tower. These effects not only reduce aerodynamic performance but also shorten the tower's fatigue life.

In this context, the hybridization approach emerges as a particularly promising solution by leveraging the coupling between WEC dynamics and the FOWT [10]. Hybrid Wind-Wave System (HWWS) has been recognized as an innovative approach to addressing stability challenges in FOWTs while enhancing overall energy availability [11]. The dynamic interaction between the WEC and the platform directly influences the dynamic response of the HWWS, which can be leveraged for motion suppression and load mitigation, ultimately improving both the structural resilience of the system and its energy efficiency. Beyond this, other advantages include energy accessibility in locations where wind and wave potential are not necessarily correlated, combined maintenance, and the possibility of sharing infrastructure [12].

Essentially, a HWWS consists of a floating platform, such as a spar, semi-submersible, tension leg platform, or barge [13]; a horizontal-axis wind turbine, such as the NREL 5MW [4], DTU 10MW [14], or IEA 15MW [15]; one or more WECs attached to the floating platform, such as Wave Star [16], Torus [17], or point absorbers; and mooring cables [18].

Some widely cited examples in the literature of HWWS include the Spar-Torus Combination (STC) [19]–[22] and the Semi-Submersible with a Flap type WEC Combination (SFC) [23]–[25]. The P80 [26], from the Danish company Floating Power Plant, which is the only commercial-stage HWWS, to the best of the authors' knowledge. Other typical topologies include OWC-barge combinations [27], [28], W2Power [29], TPL-point absorbers [30], [31], and WindWaveFloat [32].

A growing body of research highlights the potential of co-optimising the control strategies of the WECs' Power Take-Off (PTO) systems and the WT controllers within HWWSs [11], [33], [34]. Rather than treating these subsystems independently, integrated control approaches aim to exploit their dynamic coupling to achieve platform motion suppression, structural load mitigation, and improved energy efficiency. Such frameworks often combine conventional WT strategies, such as PI-based pitch control and LQR-based torque control, with advanced PTO control schemes including semi-active damping, model predictive control, or impedance matching. These approaches enable the modulation of WEC forces in synchrony with WT dynamics, allowing for the redistribution of energy and structural responses across the system. The synergy between the aerodynamic and hydrodynamic damping mechanisms introduced by this joint control can significantly enhance the overall stability and operational robustness of floating offshore wind platforms under complex environmental conditions.

This paper aims to consolidate recent findings in the domain of hybrid control for FOWT–WEC systems, bridging the gap between structural dynamics and coordinated control synthesis. Section II reviews conventional control methods for floating wind turbines. Section III presents a fully coupled aero–hydro–servo–mooring formulation, including both a multibody non-linear model and its corresponding linearised dynamic representation for a HWWS, whereas Section IV focuses on passive damping strategies, particularly the application of Tuned Mass Dampers (TMDs). Section V offers a comparative overview of HWWS topologies and control-performance outcomes and also presents typical configurations and control frameworks reported in the literature. The concluding remarks in Section VI highlight the challenges and future perspectives in this evolving field.

II. Traditional Wind Turbine Controllers

This section presents the most commonly used controllers for FOWTs. Control systems are essential for wind energy systems as wind is an uncontrollable and highly variable resource. This variability introduces complexities in power conversion and grid integration. To address these challenges, WT control systems perform key functions, including adjusting the blade pitch angle to regulate power and loads, controlling generator torque to maximise energy capture, and managing grid integration. Additionally, yaw control ensures optimal turbine orientation relative to wind direction, further enhancing efficiency and stability.

The Baseline Controller [4] and the ROSCO [3] represent two distinct approaches to WT control, with significant differences in complexity and optimization. The Baseline Controller employs a simple, predefined strategy, relying on a cubic law for torque control below rated wind speeds and a PI pitch control above rated conditions. This method, while effective for standard simulations, lacks adaptability and advanced tuning capabilities, leading to suboptimal performance in varying wind conditions.

For a better understanding of the control system of a WT, it is necessary to distinguish the regions of typical operations related to wind speed. Figure 1 shows the typical operational characteristics of a WT separated by region. The control implementation can be summarised as follows: In region 1, the wind speed is below the cut-in velocity, and connecting the WT to the grid in this condition is not beneficial because the system's losses exceed the generated power production in this region. In region 2, Maximum Power Point Tracking (MPPT) algorithms are usually applied to harvest wind power. In region 3, blade pitch control is typically applied to protect the system from elevated mechanical stress at high wind speeds, limiting power production to the rated power. Finally, in region 4, the WT is disconnected from the grid for safety reasons.

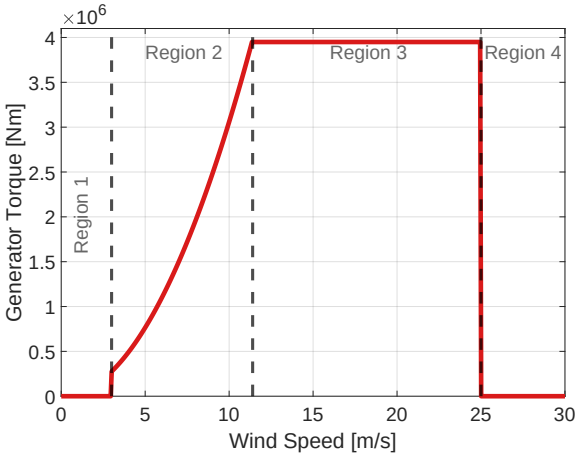

Fig. 1: Typical torque curve of a WT: regions 1 and 4 - the WT is out of operation; region 2 - MPPT algorithms applied to maximise power production; region 3 - power production is limited via pitch control. It is the torque curve for reference turbine, NREL5MW [4]. Source: Elaborated by the authors according to [3].

Pitch control is usually applied in region 3 to avoid excessive structural loads and to maintain power generation around the rated value. The aim is to maintain torque constant while applying collective pitch control to regulate the generator speed. Usually the blade pitch controller is a PI controller described as

$$\beta_c(t) = K_p \omega_e(t) + K_i \int_0^t \omega_e(\tau) d\tau, \tag{1}$$

where ω_e represents the rotor speed error calculated based in the desired rotor speed, K_p and K_i are the proportional and integral gains, respectively, and β_c is the pitch angle.

In collective pitch control, it is assumed that all the blades have the same characteristics and are subjected to the same hydrodynamic loads, which in practice is not usually the case. Thus, advanced techniques aiming to individually control each blade have been presented [35]–[39].

Another important characteristic of WTs is that, due to the variability of the source, power electronics technologies play a significant role in controlling the injection of wind power into the grid. The primary goal is to ensure the quality of the energy, even in the presence of intermittent winds, by avoiding harmonics, high transients, and frequency variations (in the absence of winds). In this regard, converters play a central role in the control strategy, and the type of generator used in the conversion system determines its operation. For a comprehensive study on the topic of WT control and the main conversion systems, including the main types of generators and their characteristics refer to [40].

In this context, electronic power converters have increasingly become more versatile, enabling the connection of variable-speed wind turbines to the grid. They achieve this by generating the desired voltage and frequencies, and effectively controlling the generated torque as well as the active/reactive power produced by the generator. The authors in [1] highlight that WT torque control is achieved through a two-layered controller: an inner loop characterised by the electronic power converter and other solid-state devices, which receives the torque set-point from the external control loop, and the external control loop that determines the torque set-point through MPPT.

The MPPT strategies involve maintaining the WT at its optimal operating point while minimising loads, incorporating various approaches:

- *Optimal torque control*: Equations (2) to (5) describe, respectively, the power extracted from the wind, the speed ratio, a quadratic law for torque in an optimal torque control MPPT approach, and the aerodynamic constant for a given wind turbine. Here, k is related with the constructive characteristic of each WT, C_p is the power coefficient which depends of the pitch angle and on the speed ratio, R represents the rotor radius, and λ the speed ratio, ρ is the air density, A is the rotor swept area, and v is the wind speed. The power coefficient is maximum $C_{p,opt}$ for a predetermined pitch angle (β_{opt}) and optimal speed ratio (λ_{opt}). When operating in region 2, it is necessary to adjust the WT rotor speed to match the changing wind speed in order to maintain the optimal tip speed ratio, thereby ensuring maximum power production.

$$P_w = \frac{1}{2}\rho A C_p v^3, \tag{2}$$

$$\lambda = \frac{\omega R}{v}, \tag{3}$$

$$\tau_g = k\omega^2, \tag{4}$$

$$k = \frac{1}{2}\rho\pi R^5 \frac{C_{p,opt}}{\lambda_{opt}^3}, \tag{5}$$

- *Power signal feedback*: It relies on real-time monitoring of the power output and adjusts the turbine's operation accordingly. It essentially follows the same operational trajectory as optimal torque control but employs a power control loop instead of directly modifying the torque. By continuously assessing the power signal, it can fine-tune the turbine's parameters to optimize energy capture under varying wind conditions.
- *Hill-climb search*: It employs an iterative approach, incrementally adjusting control parameters to ascend the power curve and reach the peak power point. It mimics a trial-and-error process, searching for the optimal operating conditions.
- *Sliding mode control*: It is a non-linear control method that employs a dynamic control approach that seeks to maintain the system within a predefined sliding surface [41], [42]. This method is known for its ability to adapt to changing conditions and disturbances, ensuring stable performance even in challenging wind environments.

Conversely, ROSCO employs advanced control strategies, such as optimal gain tuning and state-based adaptations, to improve efficiency and mitigate structural loads. By leveraging an LQR-based torque controller alongside a refined PI pitch controller with additional filtering mechanisms, ROSCO enables smoother transitions and minimizes mechanical stress. The incorporation of dynamic gain adjustments and filtering techniques enhances performance under turbulent wind conditions, making it a more adaptable and resilient solution for real-world WT applications compared to the conventional Baseline Controller. Moreover, ROSCO offers peak shaving and floating feedback functionalities, which are particularly beneficial for floating offshore wind turbines, ensuring better stability and load distribution in dynamic ocean environments.

According to Xue et al. [11], peak shaving facilitates a balance between power generation and load reduction, contributing to the mitigation of platform pitch motion. A minimum blade pitch angle is required to shave the peak of the rotor thrust curve, ultimately reducing peak tower base loads when the WT operates near its rated conditions. The rotor thrust is defined as:

$$T_r(\nu) = \frac{1}{2}\rho A v^2 C_t(\lambda, \beta), \tag{6}$$

where $C_t(\lambda, \beta)$ represents the rotor thrust coefficient, while the remaining variables are defined as previously. $C_{t,\max}(v)$ denotes the maximum allowable thrust and can be obtained from Eq. (6) when a maximum permissible rotor thrust is specified:

$$T_{r,\max} = p_{spercent} \max\left(T_r(\nu)\right), \tag{7}$$

Since both the maximum rotor thrust coefficient, $C_{t,\max}$, and the maximum speed ratio, λ, are functions of v, a minimum blade pitch angle can be defined based on a wind speed estimate. The resulting tower load reduction, which mitigates platform pitch motion, is achieved through an FOWT-specific feedback loop. In the case of ROSCO, this loop is incorporated into the blade pitch control signal and is based on the filtered tower-top acceleration:

$$\beta_c(t) = K_p\omega_e(t) + K_i\int_0^t \omega_e(\tau)d\tau + K_{float}\Delta\dot{x}_t, \tag{8}$$

here, K_{float} is a proportional gain based on floating feedback and x_t is the tower-top position in the fore-aft direction. Figure 2 illustrates the logic of the ROSCO controller.

III. Coupled Dynamic Model

Figure 3 illustrates a typical workflow adopted in control-oriented studies of HWWS. The process begins with system definition, which involves the selection of platform geometry, WT and WEC types, as well as the simulation software, capable of modelling coupled multi-physics interactions. A full system model is then developed, incorporating aero-hydro-servo-mooring dynamics and the integration of WEC components into the floating structure.

Once established, the model is typically validated through free-decay tests to capture natural frequencies, and more commonly, via numerical comparison with industry-standard tools such as OpenFAST [43], [44]. This validation step ensures the reliability of the simulation environment for subsequent control design. The linearisation phase follows, simplifying the non-linear dynamics around operating points to enable controller synthesis. The PTO controller design stage involves the selection of a suitable strategy (e.g., semi-active, MPC, impedance-matching, linear-damping), inclusion of physical constraints such as passivity and actuator limits, and formulation of a performance-based cost function. Finally, the system is evaluated through simulations under various environmental conditions, regular and irregular wave fields, and below- to above-rated wind speeds. Platform motion and power production are assessed through time-series analysis, Response Amplitude Operators (RAOs), and spectral/statistical methods, considering configurations without WECs, with passive WECs, and with actively controlled PTO systems.

Hongzhong Zhu [45] presents both a full multibody non-linear model and a linearised dynamic model for a HWWS, composed of a FOWT and multiple WECs. The system dynamics are captured through a fully coupled aero–hydro–servo–mooring formulation. Each body is considered rigid and subject to six Degrees of Freedom (DOFs). The non-linear equations of motion for the i-th body are expressed as:

$$\dot{\eta}_i = J(\eta_i)v_i, \tag{9}$$

$$\begin{aligned} &M_{RB_i}\dot{v}_i + \left(C_{RB_i}(v_i) + C_{A_i}(v_i)\right)v_i + \\ &\quad\sum_{j=1}^{4}\left(A_{ij}(\infty)\dot{v}_j + \int_0^t K_{ij}(t-\tau)v_j(\tau)d\tau\right) \\ &\quad + D_v v_i + D_q v_i|v_i| + g(\eta_i) = \tau_{m_i} + \tau_{w_i} + \tau_{a_i}, \end{aligned} \tag{10}$$

where v_i is the velocity in the body frame, η_i is the position and orientation in the inertial frame, $J(\cdot)$ is the Jacobian transformation matrix, M_{RB} the rigid-body inertia, C_{RB} and C_A the Coriolis-centripetal matrices, $A(\infty)$ the added mass

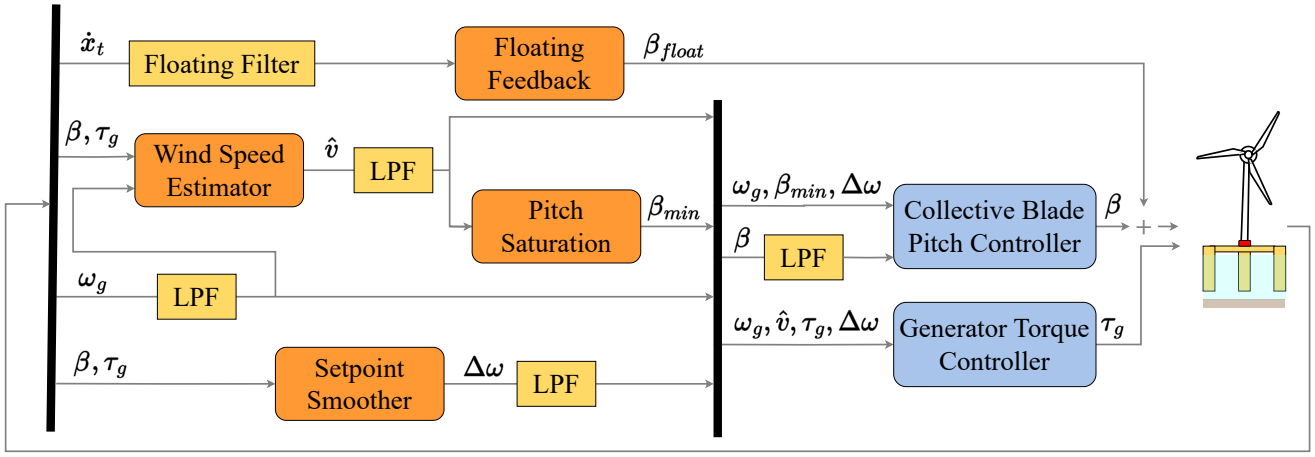

Fig. 2: Block diagram of the ROSCO controller, illustrating the interaction between various control modules. Feedback signals include the tower-top fore–aft velocity (x_t), collective blade pitch angle (β), generator speed (ω_g), and generator torque (τ_g). Key components include the *Floating Filter*, *Wind Speed Estimator*, *Pitch Saturation*, and *Set point Smoother*, along with *Low-Pass Filters (LPF)* for signal processing. The *Collective Blade Pitch Controller* and *Generator Torque Controller* regulate the blade pitch angle (β) and generator torque (τ_g), ensuring optimal WT operation. The floating feedback mechanism contributes to pitch control adjustments, enhancing stability in FOWTs. Source: adapted from [3].

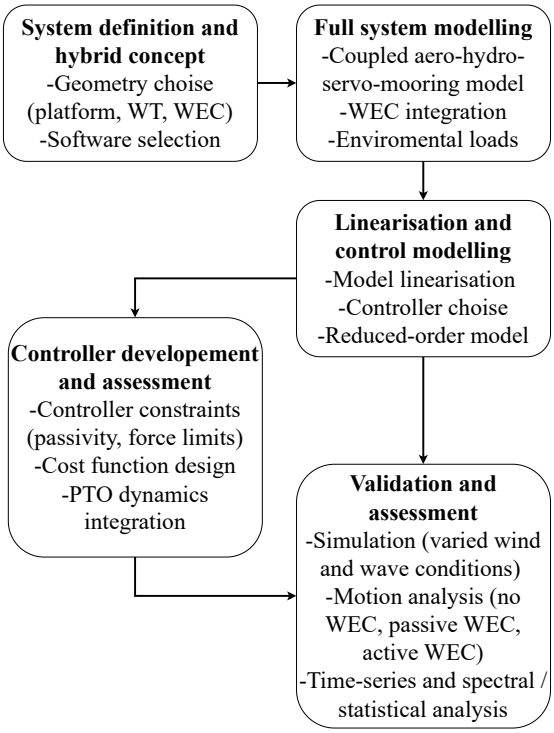

Fig. 3: Typical workflow for hybrid wind/wave systems control-oriented studies. Source: elaborated by the authors.

at infinite frequency, $K(t)$ the retardation function representing fluid-memory effects, $D_v v$ and $D_q v|v|$ are the damping forces, and $g(\eta)$ is the restoring force.

To reduce computational effort, the convolution integral is approximated as a linear system:

$$\dot{x}_r(t) = A_r x_r(t) + B_r \dot{v}(t), \tag{11}$$

$$\int_0^t K(t-\tau)v(\tau)d\tau = C_r x_r(t), \tag{12}$$

where x_r is the internal state vector identified through system identification techniques.

The wave excitation force is modelled via force RAOs as:

$$\tau_{w_i} = \sum_{j=1}^{N} |\Gamma_i(\omega_j)| \sqrt{2S(\omega_j)\Delta\omega} \cdot \cos\left(\omega_j t - \kappa_j(x_i \cos\beta + y_i \sin\beta) + \angle\Gamma_i(\omega_j) + \epsilon_j\right), \tag{13}$$

where Γ_i is the complex RAO, $S(\omega)$ the wave spectrum, κ is the wave number, and ϵ_j the random phase.

The aerodynamic loads are computed using the thrust and torque coefficients:

$$F_t = \frac{1}{2}\rho_a \pi R^2 C_t(\lambda, \beta)(v_{wx} - v_{hx})^2, \tag{14}$$

$$T_R = \frac{1}{2}\rho_a \pi R^3 \frac{C_p(\lambda, \beta)}{\lambda}(v_{wx} - v_{hx})^3, \tag{15}$$

where C_t and C_p are the thrust and power coefficients, λ is the tip-speed ratio, ρ_a is the air density, and β is the blade pitch angle.

The mooring system is implemented via MAP++ [46] as a static catenary model, while the cables connecting each WEC to the foundation are modelled as spring-damper elements:

$$F_m = \begin{cases} 0, & \text{if } d_m \leq l_m, \\ -K_s(d_m - l_m) - D_s\dot{d}_m, & \text{if } d_m > l_m, \end{cases} \tag{16}$$

where K_s and D_s are the stiffness and damping of the cable, d_m the stretched distance, and l_m the rest length.

Each WEC applies a vertical force through its PTO system, expressed as:

$$f_{p_i} = -kz_{p_i} - c\dot{z}_{p_i} - f_i(\dot{z}_{p_i}), \tag{17}$$

where z_{p_i} is the piston displacement, k and c the restoring coefficient and damping coefficient, respectively; and f_i the control force used for tuning the coupling between the FOWT and WECs.

To enable optimal controller synthesis, the nonlinear coupled dynamics of the HWWS are linearised around an operating point using a state-space representation. The linearised model includes the platform motion, mooring effects, and the dynamic interaction with the PTO-controlled WECs. The general structure of the model is given by:

$$(M + A_a)\ddot{\xi} + \Lambda\dot{\xi} + G\xi = \tau_{\text{ext}} + \Delta f, \tag{18}$$

where ξ is the vector of generalised platform and WEC displacements, M is the mass matrix, A_a is the added mass matrix, Λ is the damping matrix, and G is the hydrostatic

restoring matrix. The term τ_{ext} includes external disturbances such as wave and wind loads, while Δf is the control input vector corresponding to the WEC PTO forces.

The control inputs f are applied via a transformation matrix Δ, which maps the PTO control forces of each WEC into the global system coordinates, accounting for their spatial distribution on the floating platform. The model is typically discretised for use in predictive control applications.

To capture the control effect of the WECs, the PTO control force is included in the state-space formulation. The full system dynamics can then be expressed in discrete-time as:

$$x(k+1) = Ax(k) + Bf(k), \tag{19}$$

$$y(k) = Cx(k), \tag{20}$$

where $x(k)$ is the state vector at time step k, $f(k)$ is the control input (PTO force), and $y(k)$ represents the measured outputs of interest (e.g., platform pitch, platform heave, platform surge). The matrices A, B, and C are derived from the linearisation process and depend on the system operating point and environmental conditions.

A. Typical Software and Tools

The modelling process outlined in the previous sections typically requires the solution of complex partial differential equations, which rarely admit analytical solutions. As a result, computational implementation becomes essential to obtain numerical approximations. Consequently, the choice of appropriate software and tools plays a critical role in the modelling of dynamic systems. Table I provides a selection of commonly used software packages in this context. Rather than presenting an exhaustive list of all available tools, the aim is to highlight those most frequently referenced in the literature.

IV. Passive Control Devices

TMDs have emerged as a promising passive control strategy to mitigate undesirable structural vibrations in FOWTs [63], [64]. These devices comprise a secondary mass connected to the main structure via a spring-damper system, tuned to a specific frequency associated with critical structural modes, such as tower fore-aft or platform pitch. When properly tuned, the TMD absorbs vibrational energy by resonating out of phase with the primary structure, thereby reducing the amplitude of motion and associated fatigue loads. TMDs offer a cost-effective and reliable solution for attenuating dynamic responses without the need for active control or additional power input. Their integration can enhance the operational lifespan of key components, improve overall platform stability under turbulent environmental conditions, and complement other wind turbine control strategies. Recent studies have shown that well-designed TMDs can significantly reduce tower-top accelerations and nacelle displacements, particularly under resonance-prone conditions in the low-frequency range typical of floating platforms.

A classical example of this approach is the study by Galán-Lavado and Santos [65], in which the authors investigate the influence of TMD placement on vibration reduction performance for a barge-type FOWT, using the NREL 5-MW reference turbine model and the FAST simulation platform. They evaluate configurations with one or two TMDs, systematically varying their positions along the fore–aft and side–side directions of the floating platform.

The dynamic behaviour was modelled via Lagrangian mechanics, yielding a reduced 2-DOF representation, where the main state variables are the platform pitch angle θ_p and tower bending angle θ_t. The linearised equations of motion used for small angular displacements are:

$$\begin{aligned} I_t\ddot{\theta}_t &= m_t g R_t \theta_t - k_t(\theta_t - \theta_p) - d_t(\dot{\theta}_t - \dot{\theta}_p) \\ &\quad - m_t g R_t \theta_t - k_t R_t^2 \theta_t - d_t R_t^2 \dot{\theta}_t, \\ I_p\ddot{\theta}_p &= -d_p\dot{\theta}_p - k_p\theta_p - m_p g R_p \theta_p \\ &\quad + k_t(\theta_t - \theta_p) + d_t(\dot{\theta}_t - \dot{\theta}_p). \end{aligned} \tag{21}$$

here, I_t and I_p represent the moments of inertia of the tower and the platform, respectively. The parameters m_t and m_p refer to the effective masses at the tower top and the platform, while R_t and R_p denote the distances from the respective centres of mass to the pivot point of rotation. The terms k_t and k_p correspond to the rotational stiffness coefficients of the tower and platform, and d_t and d_p are their respective damping coefficients. Finally, g is the gravitational acceleration. Together, these parameters define the coupled rotational dynamics between the tower and the floating platform, allowing for an analysis of the vibration mitigation achieved through the integration of passive damping devices.

Results showed that platform-mounted TMDs can effectively reduce both the tower-top displacement and platform pitch angle, key indicators of structural stress. Notably, optimal placement of a single TMD was found to be slightly upwind of the tower base, with the suppression rate of tower-top standard deviation exceeding 30%. The platform-based configuration offers a distinct advantage over nacelle-based solutions due to fewer mass and volume constraints, allowing the use of heavier dampers for greater vibrational energy dissipation. To illustrate the concept of TMDs, Figure 4 presents an implementation of a tuned mass damper.

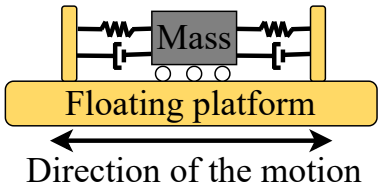

Fig. 4: A passive TMD mounted on a FOWT. Source: Elaborated by the authors.

Passive control methods are highly effective within their targeted frequency range and offer a low-cost, maintenance-free means of enhancing the stability of FOWTs. They also provide a solid foundation for the development of hybrid configurations that integrate WECs or semi-active control systems. However, their effectiveness may diminish under environmental variability and system parameter uncertainties [66]. As an alternative, the control of the WEC's PTO system-capable of actively responding to dynamic conditions-is explored in the following sections.

V. Integrated Control Optimization for Wind Turbines and PTO-WEC Systems

In this section, we demonstrate various combinations of FOWTs and WECs and analyze how PTO-WEC control influences the overall system performance. Specifically, we evaluate the impact on platform motion, structural loads, nacelle acceleration, and power output variability, highlighting both the benefits and trade-offs of integrated wind-wave energy systems.

The control scheme illustrated in Figure 5 presents an architecture for HWWS, where the control of the WT and the PTO unit of the WEC are co-ordinated to enhance platform stability and optimise energy production. The system operates under varying environmental conditions, using wind and wave inputs to drive a multi-loop control framework.

TABLE I: Typical Software and Tools

Software	Applicability	Description	Ref.	Software	Applicability	Description	Ref.
Ansys	AHSE tools	Widely used software suite for engineering simulation and finite element analysis.	[47]	Profoil	Airfoil design	Inverse design tool for airfoil geometry based on aerodynamic constraints.	[48]
Capytaine	Hydrodynamic analysis	Linear potential flow solver.	[49]	Propid	Aerodynamic design	Inverse design tool for rotor blade geometry and performance.	[50]
F2A and Catifes	AHSE tools	Combines FAST with Ansys Aqwa's numerical capabilities.	[51]–[53]	Wamit	Hydrodynamic analysis	Frequency-domain solver for wave-body interactions on offshore structures.	[54]
Most	FOWT Simulation Tool	Design-phase tool for modelling floating platforms, WT aerodynamics, generators, and control laws.	[55]	WECSim	WEC simulator	MATLAB/Simulink-based tool for modelling WECs, mooring, yawing, and hydrodynamics.	[56]
Nemoh	Hydrodynamic analysis	Linear potential flow solver.	[57], [58]	WindIO	WT/wind farm MDAO	Multi-language library for I/O in wind turbine and wind farm MDAO.	[59]
OpenFAST	AHSE tools	NREL-developed tool for wind turbine simulation, including fatigue, aerodynamics, structures, and turbulence.	[43], [44]	WISDEM	Integrated WT analysis	NREL-developed; cost and performance analysis of wind turbines using OpenMDAO.	[60]
OrcaFlex	Integrated analysis	AHSE tool for marine systems under various load conditions.	[61]	WEIS	FOWT Simulation Tool	Open-source tool for FOWT design and analysis, integrating AHSE modelling with multidisciplinary design optimisation (MDO).	[62]

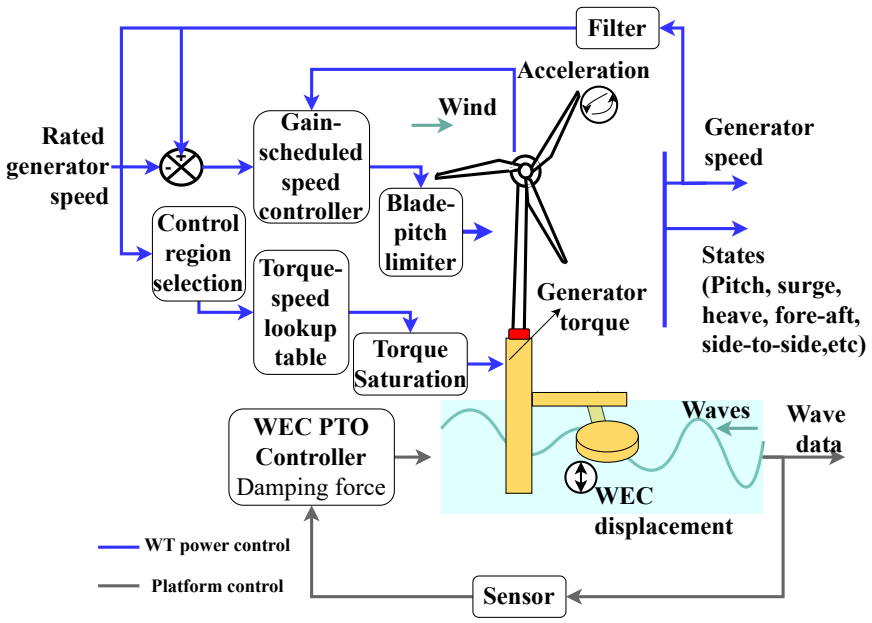

Fig. 5: Block diagram of a coupled control architecture for a HWWS, where the PTO control of the WEC is designed to assist the FOWT control strategy. The system integrates region-specific wind turbine control (torque/pitch) with a feedback-based WEC controller, aiming at load mitigation, platform motion suppression, and overall energy performance improvement. Source: Elaborated by the authors.

On the WT side, generator speed and platform acceleration are processed through filters and compared against a lookup table to define the appropriate control region (below-rated, rated, or above-rated). A gain-scheduled speed controller is then engaged, followed by a blade pitch limiter and torque saturation mechanism to regulate generator torque accordingly.

Simultaneously, the WEC displacement, measured via sensors and often associated with platform motion, is fed into a dedicated PTO controller. This controller modulates the damping force applied by the WEC to attenuate platform oscillations, thus mitigating structural loads and platform motion. The interaction between aerodynamic and hydrodynamic forces is captured through a coupled set of platform states, including pitch, surge, heave, and other DOFs. This coupling enables advanced control strategies where both energy harvesting and motion suppression objectives are pursued jointly, illustrating the potential of HWWS to improve power quality and reduce fatigue loads on floating structures.

Figure 6 showcases a range of typical HWWS configu-

rations found in the literature. These concepts reflect the diversity in integrating WECs with FOWTs. The designs vary in platform type, ranging from spar-buoy and semi-submersible to Tension-Leg Platforms (TLPs), and in the WEC technologies employed, including point absorbers, flap-type converters, and Oscillating Water Columns (OWCs). These hybrid arrangements illustrate the versatility in combining wind and wave energy capture, with strategic placement of WECs around or beneath the FOWT structure.

A. Integrated Approaches to Platform Dynamics, Fatigue Management, and Power Generation in HWWSs

1) Integration of Barge and Oscillating Water Column: A recent contribution by Aboutalebi et al. [70] addresses the challenge of mitigating platform oscillations and power fluctuations in barge-type FOWTs by integrating four OWCs into the platform structure. The novelty lies in a switching control strategy applied to the OWC valves, aiming not at maximising wave energy extraction but at damping undesirable dynamics in the platform motion. The controller operates by evaluating the RAOs of platform pitch for different wind regimes and uses this frequency-domain characterisation to dynamically modulate the airflow through the OWCs, thus suppressing wave-induced resonance.

The equations of motion for the coupled wind–wave–structure system are formulated both in time and frequency domains, incorporating added mass, hydrodynamic damping, and stiffness contributions, as well as the effects of the PTO system. In the frequency domain, the control-oriented model is described by:

$$I(\omega)\ddot{x} + (B(\omega) + B_{\text{PTO}}(\omega))\dot{x} + (K + K_{\text{PTO}}(\omega))x = f_{\text{ext}}(\omega),$$

where the PTO elements are derived from a linearised isentropic air compression model. The switching controller, governed by a sigmoidal function of wave period, opens or closes the OWC valves based on the crossing point of RAO curves, which varies with wind speed. This control scheme is further complemented by pitch angle regulation and generator torque control, employing a variable-speed strategy for optimal energy conversion.

Simulation results reveal that the proposed control approach significantly reduces structural oscillations and power variability across below-rated, rated, and above-rated wind speeds. In below-rated conditions, the pitch motion was reduced by 33%, fore-aft displacement by 28.5%, and power fluctuations by 26.6%. Similar reductions were observed in other scenarios, with up to 30% improvement in pitch stability. Notably, the controlled system also achieved slightly higher average power generation, suggesting that damping-induced stability can indirectly enhance aerodynamic performance.

2) Integration of OC4 DeepCwind Semisubmersible FOWT with Point Absorbers and Linear Damping Controller: Xue et al. [11] implemented an integration of the OC4 DeepCwind Semisubmersible FOWT, equipped with a 5 MW wind turbine and three point absorber WECs inspired by a wave star shape. They analysed the effect of applying a PTO-WEC Linear Damping Controller (LDC) , described through Eqs. (22) to (24), compared to baseline and ROSCO wind turbine controllers on the floating platform dynamics under various wind conditions and sea states.

$$\tau_{PTO} = B_{PTO}\omega_{arm}, \tag{22}$$

$$P_{WEC} = \tau_{PTO}\omega_{arm}, \tag{23}$$

$$\omega_{arm} = \dot{\theta}, \tag{24}$$

The equations describe the transformation of heave-induced buoy motion into rotational motion around a hinge, which is linked to a hydraulic PTO system. This PTO operates linearly, with the generated torque (τ_{PTO}) being directly proportional to the arm's angular velocity (ω_{arm}), scaled by a damping coefficient (B_{PTO}). Consequently, the power extracted from the waves (P_{WEC}) is obtained by multiplying the PTO torque by the angular velocity. The angular speed of the arm is defined as the time derivative of the angular displacement (θ), which itself is derived from the hinge kinematics. Specifically, θ is computed using the arcsine of the cross-product between two vectors: one extending from the hinge to the WECs center of gravity and the other reaching from the hinge to the platform's center of gravity.

The presence of uncontrolled WECs amplifies platform motion in dominant wind frequency regions, whereas applying PTO-WEC control suppresses motion in wave-dominated frequencies. Additionally, integrating WECs with the FOWT reduces the tower-base fore-aft bending moment caused by wave forces, except when the excitation wave frequency aligns with the WEC resonance frequency. A similar trend is observed in wind turbine nacelle acceleration in the fore-aft direction: while baseline and ROSCO controllers alone have little impact, WEC integration reduces nacelle acceleration in frequency regions outside the WEC resonance. However, this reduction is only marginally different between cases with and without WECs attached. Regarding power output, improvements between 2.2% and 4.7% were observed across different design load cases, though this came with increased power output variability. In one out of four cases, a 1.8% power penalty was noted, highlighting a trade-off between performance gains and output stability.

3) Integration of DeepCwind Semisubmersible FOWT with Heaving-Type WEC and Bang-Bang Control: Another notable result in the literature considers the application of LDC control, similar to the previous case, but with an adaptive damping coefficient that varies according to the platform's motion. This approach is referred to as bang-bang control (BBC). Chen et al. [71] investigated the application of BBC on three cylindrical-shaped WECs attached to a DeepCwind platform. A bang-bang controller is typically a two-step on-off controller that switches abruptly between two states. In this case, it required only knowledge of the HWWS motion responses without the need for wave prediction.

In the referenced paper, LDC was applied, and the two switching states were selected based on the values of the linear damping coefficient used in LDC. One of the damping coefficients was chosen as the optimal PTO damping, defined as $B_0 = B_{hydro}$, where B_{hydro} is the frequency-dependent hydrodynamic damping associated with the power dissipation of radiated waves. The second damping value was set to be twice that of B_0:

$$B_{\text{PTO}} = \begin{cases} B_0, & \dot{\theta}_P RV_1 < 0, \\ 2B_0, & \dot{\theta}_P RV_1 \geq 0, \end{cases} \tag{25}$$

where, $\dot{\theta}_p$ is the platform pitch velocity, and RV_1 is the relative velocity between the WEC and the platform.

The LDC control law was defined as follows:

$$F_{\text{PTO}} = B_{\text{PTO}}\Delta\dot{x}, \tag{26}$$

where x represents the WEC displacement relative to the platform.

The results demonstrated a reduction in pitch and heave motions of the platform by up to 17.1% and 34.6%, respectively. Additionally, power production increased by approximately 6%, while tower-base fatigue was reduced by 11.21% when comparing the HWWS configuration to the standalone FOWT. Furthermore, it was found that BBC is superior in terms of platform motion suppression compared to LDC.

B. LCOE-Focused Co-Design of Hybrid Wind-Wave Systems

Faraggiana et al. [72] propose a methodology for the design, modelling, and optimisation of a novel HWWS

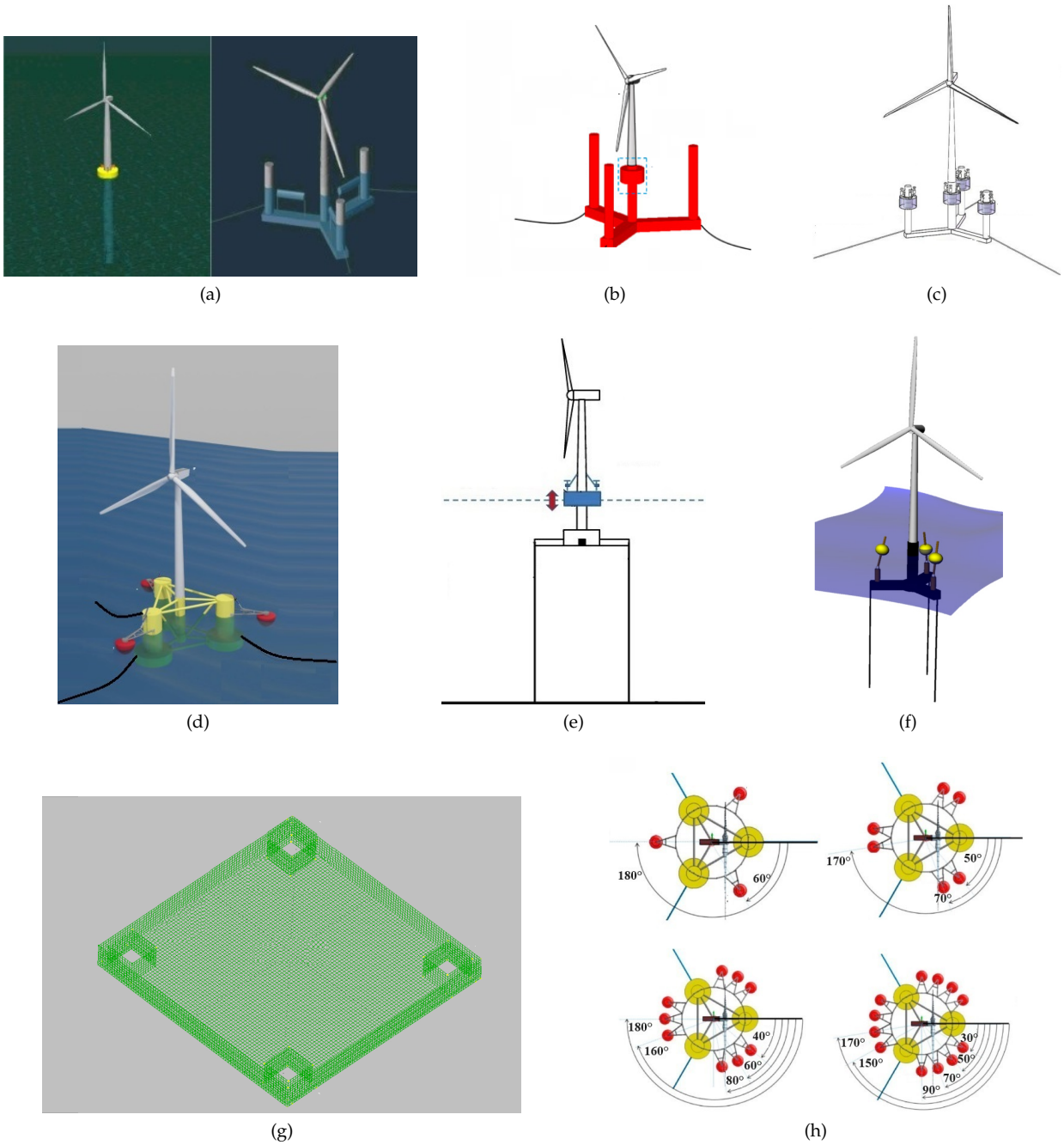

Fig. 6: Typical wind-wave system combinations: (a) The Spar-Torus and Semi-submersible-Flap combination concepts. Source: adapted from [17]. (b) A 5 MW semi-submersible FOWT with a Torus-type WEC at the centre. Source: adapted from [67]. (c) A semisubmersible platform with multiple heave oscillating WECs at each of its columns. Source: adapted from [68]. (d) A semisubmersible with three point-absorbers. Source: adapted from [33]. (e) A TLP-type floating wind turbine and a heave-type WEC. Source: adapted from [30]. (f) A TLP-type floating wind turbine and three point-absorbers. Source: adapted from [31]. (g) Typical topology of four OWCs combined with a barge platform. Source: adapted from [27]. (h) Wavestar WEC with multi-point-absorber around DeepCwind semisubmersible floating platform. Source: adapted from [69].

aimed at reducing the LCOE. The system integrates a semi-submersible floating platform equipped with the NREL 5 MW WT and three WaveStar-type point absorber WECs.

The methodology comprises a four-step framework. First, hydrodynamic and structural design of the WEC arms is achieved through geometric optimisation, constrained by a hydrostatic balance condition:

$$F_{NB_{\text{arm}}} x_{\text{arm}} + F_{NB_{\text{float}}} x_{\text{float}} = M_{\text{arm}} g x_{\text{arm}} - (B_{\text{float}} - M_{\text{float}} g) x_{\text{float}}. \quad (27)$$

Second, dynamic simulation is conducted in the time domain using `MOST` [55], which integrates the hydrodynamic solver `Nemoh`, Blade Element Momentum Theory (BEMT) for aerodynamic loads, and look-up tables for mooring and wind effects. The PTO of the WECs is modelled via either a linear damper-spring mechanism:

$$T = c_{\text{PTO}} \dot{\theta} + k_{\text{PTO}} \theta, \quad (28)$$

or a more realistic nonlinear hydraulic PTO, including bidirectional pistons and accumulator chambers.

Third, a two-stage optimisation strategy is employed. A genetic algorithm, assisted by Kriging-based surrogate models, identifies promising regions in the design space. These are refined using local optimisation via the Nelder–Mead

method. The cost-performance trade-off is captured through the objective function:

$$f_{\text{cost}} = \frac{C_{\text{platform}} + C_{\text{PTO}}}{E_{\text{WECs}}}, \tag{29}$$

where C denotes capital costs and E is the annual energy output.

Finally, the LCOE is calculated as:

$$\text{LCOE} = \frac{C_0 + \sum_{i=1}^{n} \frac{O}{(1+r)^i} + \frac{D}{(1+r)^n}}{\sum_{i=1}^{n} \frac{E}{(1+r)^i}}, \tag{30}$$

where C_0 is the capital expenditure, O the annual operating costs, D the decommissioning costs, E the yearly energy production, and r the discount rate.

The hybrid system demonstrates a total power increase of approximately 14.3% relative to the standalone FOWT, comprising a 6.8% improvement from enhanced turbine performance and a 7.5% contribution from the WECs under linear PTO control. When using hydraulic PTOs, the WEC energy contribution drops to 2.6%, although this configuration significantly reduces the power fluctuation ratio (PFR):

$$R_f = \frac{P_{\text{high}} - P_{\text{low}}}{P_{\text{rated}}}. \tag{31}$$

The LCOE is reduced by up to 11% in optimal scenarios. Under more conservative assumptions for PTO costs and wave energy capture, the LCOE advantage narrows but remains favourable, particularly in high-energy wave climates. Breakdown of capital costs shows that the wind turbine and platform account for 49%, moorings and cables 35%, and the PTO system 12%, with the bidirectional piston comprising 54% of the latter.

From a dynamic performance perspective, the hybrid system maintains pitch angles below 15° and nacelle accelerations under 2 m/s^2 even during extreme conditions. The front-facing WECs deliver the bulk of the wave power due to wave directionality.

VI. Conclusion

Hybrid Wind-Wave Systems represent a promising frontier in offshore renewable energy, combining the aerodynamic efficiency of FOWTs with the inherent damping and generation potential of WECs. This review has examined the evolution of control strategies employed in such systems, ranging from traditional wind turbine control schemes and passive damping techniques to more recent developments involving coupled and co-optimised controllers. Passive solutions, such as TMDs, offer low-cost improvements to stability but are limited by their sensitivity to system variability. In contrast, semi-active and active control of the WEC's PTO system allows for dynamic adaptation to environmental conditions and has demonstrated significant reductions in platform motion and structural loads.

Furthermore, the integration of WEC control within the broader FOWT control loop offers unique opportunities to balance energy extraction with load mitigation. Various studies have demonstrated that carefully tuned PTO controllers can contribute not only to stabilising the platform but also to enhancing the net power production of the hybrid system, particularly under harsh sea states where wind-only systems are typically curtailed.

The analysis of different HWWS topologies and control architectures reveals that platform type, WEC configuration, and controller design must be co-optimised to unlock the full potential of hybrid offshore platforms. Future research should prioritise experimental validation, cost-benefit assessments, and the development of unified control frameworks that seamlessly integrate wind and wave subsystems. By doing so, HWWSs could become a cornerstone of reliable, resilient, and economically viable offshore energy systems in the coming decades.

References

[1] E. J. N. Menezes, A. M. Araújo, and N. S. B. da Silva, "A review on wind turbine control and its associated methods," *Journal of Cleaner Production*, 2018.

[2] X. Wu *et al.*, "Foundations of offshore wind turbines: A review," *Renewable and Sustainable Energy Reviews*, 2019.

[3] N. J. Abbas, D. S. Zalkind, L. Pao, and A. Wright, "A reference open-source controller for fixed and floating offshore wind turbines," *Wind Energy Science*, 2022.

[4] J. Jonkman, S. Butterfield, W. Musial, and G. Scott, "Definition of a 5-mw reference wind turbine for offshore system development," *NREL Report*, 2009.

[5] R. A. Gideon and E. Bou-Zeid, "Collocating offshore wind and wave generators to reduce power output variability: A multi-site analysis," *Renewable Energy*, 2021.

[6] F. Meng *et al.*, "Co-located offshore wind–wave energy systems: Can motion suppression and reliable power generation be achieved simultaneously?" *Applied Energy*, 2023.

[7] S. Rasool *et al.*, "Quantifying the reduction in power variability of co-located offshore wind-wave farms," *Renewable Energy*, 2022.

[8] J. G. d. Silva, T. Nazaré, M. Costa, M. J. Lacerda, and E. Nepomuceno, "Engineering and technology applications of control co-design: A survey," *IEEE Access*, vol. 12, pp. 81 692–81 717, 2024.

[9] J. M. Kluger *et al.*, "A first-order dynamics and cost comparison of wave energy converters combined with floating wind turbines," in *Proceedings of the International Offshore and Polar Engineering Conference*, 2017.

[10] J. Li *et al.*, "Wind–wave coupling effect on the dynamic response of a combined wind–wave energy converter," *Journal of Marine Science and Engineering*, 2021.

[11] L. Xue, N. Y. Sergiienko, B. Ding, B. Cazzolato, Z. Wei, Y. Yang, F. Cao, H. Shi, and Y. Xue, "Control optimization and dynamic response analysis of a combined semi-submersible floating wind turbine and point-absorber wave energy converters," *Ocean Engineering*, 2025.

[12] S. Astariz, C. Perez-Collazo, J. Abanades, and G. Iglesias, "Co-located wind-wave farm synergies (operation & maintenance): A case study," *Energy Conversion and Management*, 2015.

[13] M. Barooni *et al.*, "Floating offshore wind turbines: Current status and future prospects," *Energies*, 2023.

[14] C. Bak, F. Zahle, R. Bitsche, T. Kim, A. Yde, L. C. Henriksen, M. H. Hansen, J. P. A. A. Blasques, M. Gaunaa, and A. Natarajan, "The dtu 10-mw reference wind turbine," 2013.

[15] E. Gaertner, J. Rinker, L. Sethuraman, F. Zahle, B. Anderson, G. E. Barter, N. J. Abbas, F. Meng, P. Bortolotti *et al.*, "Iea wind tcp task 37: Definition of the iea 15-megawatt offshore reference wind turbine," *NREL Report*, 2020.

[16] M. Kramer, L. Marquis, and P. Frigaard, "Performance evaluation of the wavestar prototype," in *9th EWTEC 2011*, 2011.

[17] Z. Gao *et al.*, "Comparative numerical and experimental study of two combined wind and wave energy concepts," *Journal of Ocean Engineering and Science*, 2016.

[18] K.-T. Ma *et al.*, *Mooring system engineering for offshore structures*. Gulf Professional Publishing, 2019.

[19] M. J. Muliawan, M. Karimirad, T. Moan, and Z. Gao, "Stc (spar-torus combination): a combined spar-type floating wind turbine and large point absorber floating wave energy converter—promising and challenging," in *International Conference on Offshore Mechanics and Arctic Engineering*, 2012.

[20] M. Murai and X. Liu, "Possibility of reducing spar-type fowt hydrodynamic response using a torus structure with annular flow," in *International Conference on Offshore Mechanics and Arctic Engineering*, 2021.

[21] L. Wan, N. Ren, and P. Zhang, "Numerical investigation on the dynamic responses of three integrated concepts of offshore wind and wave energy converter," *Ocean Engineering*, 2020.

[22] A. Mitra, S. Sarkar, A. Chakraborty, and S. Das, "Sway vibration control of floating horizontal axis wind turbine by modified spar-torus combination," *Ocean Engineering*, 2021.

[23] A. Neisi, H. R. Ghafari, H. Ghassemi, T. Moan, and G. He, "Power extraction and dynamic response of hybrid semi-submersible yaw-drive flap combination (syfc)," *Renewable Energy*, 2023.

[24] C. Michailides, Z. Gao, and T. Moan, "Experimental study of the functionality of a semisubmersible wind turbine combined with flap-type wave energy converters," *Renewable Energy*, 2016.

[25] Q. Li, C. Michailides, Z. Gao, and T. Moan, "A comparative study of different methods for predicting the long-term extreme structural responses of the combined wind and wave energy concept semisubmersible wind energy and flap-type wave energy converter," *Proceedings of the Institution of Mechanical Engineers, Part M*, 2018.

[26] Floating Power Plant AS, "Private communication," 2025.

[27] P. Aboutalebi, F. M'zoughi, I. Garrido, and A. J. Garrido, "Performance analysis on the use of oscillating water column in barge-based floating offshore wind turbines," *Mathematics*, 2021.

[28] L. Li, C. Ruzzo, M. Collu, Y. Gao, G. Failla, and F. Arena, "Analysis of the coupled dynamic response of an offshore floating multi-purpose platform for the blue economy," *Ocean Engineering*, 2020.

[29] J. E. Hanssen, L. Margheritini, K. O'Sullivan, P. Mayorga, I. Martinez, A. Arriaga, I. Agos, J. Steynor, D. Ingram, R. Hezari, and J. H. Todalshaug, "Design and performance validation of a hybrid offshore renewable energy platform," in *2015 Tenth International Conference on Ecological Vehicles and Renewable Energies (EVER)*, 2015.

[30] N. Ren, Z. Ma, B. Shan, D. Ning, and J. Ou, "Experimental and numerical study of dynamic responses of a new combined tlp type floating wind turbine and a wave energy converter under operational conditions," *Renewable Energy*, 2020.

[31] E. E. Bachynski and T. Moan, "Point absorber design for a combined wind and wave energy converter on a tension-leg support structure," in *International Conference on Offshore Mechanics and Arctic Engineering*, 2013.

[32] A. Weinstein, D. Roddier, and K. Banister, "Windwavefloat (wwf): Final scientific report," Tech. Rep., 2012.

[33] Y. Si, Z. Chen, W. Zeng, J. Sun, D. Zhang, X. Ma, and P. Qian, "The influence of power-take-off control on the dynamic response and power output of combined semi-submersible floating wind turbine and point-absorber wave energy converters," *Ocean Engineering*, 2021.

[34] Z. Chen, J. Sun, J. Yang, Y. Sun, Q. Chen, H. Zhao, P. Qian, Y. Si, and D. Zhang, "Experimental and numerical analysis of power take-off control effects on the dynamic performance of a floating wind-wave combined system," *Renewable Energy*, 2024.

[35] E. A. Bossanyi, "Individual blade pitch control for load reduction," *Wind Energy*, 2003.

[36] V. Petrović *et al.*, "Advanced control algorithms for reduction of wind turbine structural loads," *Renewable Energy*, 2015.

[37] M. Jelavic, V. Petrovic, and N. Peric, "Individual pitch control of wind turbine based on loads estimation," in *IECON 2008*, 2008.

[38] S. Kanev and T. van Engelen, "Exploring the limits in individual pitch control," in *European Wind Energy Conference*, 2009.

[39] K. Selvam *et al.*, "Feedback–feedforward individual pitch control for wind turbine load reduction," *Int. J. of Robust and Nonlinear Control*, 2009.

[40] M. A. Hannan *et al.*, "Wind energy conversions, controls, and applications: A review for sustainable technologies and directions," *Sustainability*, 2023.

[41] J. Mérida *et al.*, "Analysis and synthesis of sliding mode control for large scale variable speed wind turbine for power optimization," *Renewable Energy*, 2014.

[42] R. Saravanakumar and D. Jena, "Validation of an integral sliding mode control for optimal control of a three blade variable speed variable pitch wind turbine," *International Journal of Electrical Power & Energy Systems*, 2015.

[43] J. M. Jonkman, M. L. Buhl *et al.*, "Fast user's guide," 2005.

[44] "Openfast documentation," 2025.

[45] H. Zhu, "Optimal semi-active control for a hybrid wind-wave energy system on motion reduction," *IEEE Transactions on Sustainable Energy*, 2023.

[46] National Renewable Energy Laboratory (NREL), "Map++ (mooring analysis program plus plus)," 2013.

[47] E. Madenci and I. Guven, *The finite element method and applications in engineering using ANSYS*. Springer, 2015.

[48] M. Selig, "PROFOIL - a multipoint inverse airfoil design method," available at: https://github.com/m-selig/PROFOIL/blob/main/docs/PROFOIL-User-Guide-2022.pdf. Accessed on April 11th, 2025.

[49] M. Ancellin and F. Dias, "Capytaine: a python-based linear potential flow solver," *Journal of Open Source Software*, 2019.

[50] M. S. Selig, "Propid: Inverse design tool for rotors," 2025.

[51] Y. Yang *et al.*, "Development and application of an aero-hydro-servo-elastic coupling framework for analysis of floating offshore wind turbines," *Renewable Energy*, 2020.

[52] Y. Yang, J. Fu, Z. Shi, L. Ma, J. Yu, F. Fang, S. Chen, Z. Lin, and C. Li, "Performance and fatigue analysis of an integrated floating wind-current energy system considering the aero-hydro-servo-elastic coupling effects," *Renewable Energy*, vol. 216, p. 119111, 2023. [Online]. Available: https://www.sciencedirect.com/science/article/pii/S096014812301025X

[53] Y. Yang *et al.*, "Effects of tidal turbine number on the performance of a 10 mw-class semi-submersible integrated floating wind-current system," *Energy*, 2023.

[54] I. WAMIT, "Wamit: Wave analysis mit," 2025.

[55] "MOST - MATLAB for OFWT simulation tools," available in: https://morenergylab.polito.it/wp-content/uploads/2022/10/Most-User-Manual.pdf. Acessed in april 11th of 2025.

[56] S. N. Laboratories and NREL, "Wec-sim (wave energy converter simulator)," 2025.

[57] R. Kurnia and G. Ducrozet, "Nemoh v3.0 user manual," 2025.

[58] M. Penalba, T. Kelly, and J. V. Ringwood, "Using nemoh for modelling wave energy converters: A comparative study with wamit," in *12th European Wave and Tidal Energy Conference*, 2017.

[59] I. W. T. . Team, "Windio: A multi-language library for wind energy systems modelling," 2025.

[60] N. R. E. L. (NREL), "Wisdem: Wind-plant integrated system design and engineering model," 2025.

[61] Orcina Ltd., "Orcaflex help," 2025.

[62] N. R. E. L. (NREL), "Weis: Wind energy with integrated servo-control," 2025.

[63] S. Park, M. A. Lackner, P. Pourazarm, A. Rodríguez Tsouroukdissian, and J. Cross-Whiter, "An investigation on the impacts of passive and semiactive structural control on a fixed bottom and a floating offshore wind turbine," *Wind Energy*, 2019.

[64] H. Zuo, K. Bi, and H. Hao, "A state-of-the-art review on the vibration mitigation of wind turbines," *Renewable and Sustainable Energy Reviews*, 2020.

[65] A. Galán-Lavado and M. Santos, "Analysis of the effects of the location of passive control devices on the platform of a floating wind turbine," *Energies*, 2021.

[66] V. Jahangiri and C. Sun, "Three-dimensional vibration control of offshore floating wind turbines using multiple tuned mass dampers," *Ocean Engineering*, 2020.

[67] Y. Wang, W. Shi, C. Michailides, L. Wan, H. Kim, and X. Li, "Wec shape effect on the motion response and power performance of a combined wind-wave energy converter," *Ocean Engineering*, vol. 250, p. 111038, 2022.

[68] Y. Li, M. C. Ong, K. Wang, L. Li, and Z. Cheng, "Power performance and dynamic responses of an integrated system with a semi-submersible wind turbine and four torus-shaped wave energy converters," *Ocean Engineering*, vol. 259, p. 111810, 2022.

[69] H. R. Ghafari, H. Ghassemi, and G. He, "Numerical study of the wavestar wave energy converter with multi-point-absorber around deepcwind semisubmersible floating platform," *Ocean Engineering*, vol. 232, p. 109177, 2021.

[70] P. Aboutalebi, F. M'zoughi, I. Garrido, and A. J. Garrido, "A control technique for hybrid floating offshore wind turbines using oscillating water columns for generated power fluctuation reduction," *Journal of Computational Design and Engineering*, 2022.

[71] Z. Chen, J. Yu, J. Sun, M. Tan, S. Yang, Y. Ying, P. Qian, D. Zhang, and Y. Si, "Load reduction of semi-submersible floating wind turbines by integrating heaving-type wave energy converters with bang-bang control," *Frontiers in Energy Research*, 2022.

[72] E. Faraggiana, M. Sirigu, A. Ghigo, E. Petracca, G. Mattiazzo, and G. Bracco, "Conceptual design and optimisation of a novel hybrid device for capturing offshore wind and wave energy," *Journal of Ocean Engineering and Marine Energy*, 2024.